# MAGNETIC DETECTION AND TRACKING OF MILITARY VEHICLES

Peter V. Czipott[1], Alexander R. Perry[1], Brian R. Whitecotton[1], Yacine Dalichaouch[1], David O. Walsh[2], Robert T. Kinasewitz[3], Kent J. Kogler[4]

[1]Quantum Magnetics, Inc.
San Diego, CA 92121

[2]Vista Clara
Everett, WA 98204

[3]U.S. Army TACOM-ARDEC
Picatinny Arsenal, NJ 07806

[4]IITRI
Fairborn, OH 45324

## ABSTRACT

Under the Next Generation Scatterable Mines (NGSM) program led by the U.S. Army TACOM-ARDEC and as a subcontractor to IITRI, Quantum Magnetics (QM) has participated in several rounds of field experiments in magnetic detection and tracking of military vehicles. Field data were acquired by three generations of magnetoresistive (MR) magnetic tensor gradiometers and analyzed by QM and Vista Clara. Successive gradiometer design generations mark a path to meeting NGSM form factor constraints. Magnetic gradiometry can detect and unambiguously locate magnetic targets, even in magnetically contaminated environments, as shown by results presented below.

## 1.0 INTRODUCTION

Magnetic sensors can detect targets containing ferromagnetic materials because they distort the Earth's magnetic field. The magnetic field of an object can be expressed as a multipole series expansion. Since individual magnetic charges do not exist, the lowest order is the dipole, which decays as $1/r^3$. Higher-order multipoles decay with correspondingly higher powers of the distance. For measurement ranges larger than the order of the largest target dimension, the dipole moment dominates the signal, and the problem of locating and characterizing the target becomes that of locating a magnetic dipole and measuring its moment vector.

Locating a target of unknown characteristics at an unknown position requires the determination of six unknowns. Three unknowns represent the target's location, and three more represent its magnetic moment vector. Detection and characterization (in terms of magnetic moment) cannot be separated into distinct problems, but must be accomplished simultaneously. Applying different constraints to the target characteristics (for instance, foreknowledge of the target type) or to the target location (for instance, foreknowledge of the target path) can reduce the dimensionality of the problem somewhat. In this paper, we show results for an unconstrained detection, localization and characterization problem.

## 2.0 MAGNETIC SENSOR TYPES

Different magnetic sensor configurations bring different advantages and limitations to bear on the problem. Total-field sensors are immune to orientation noise in the Earth's field, but, producing only a single datum, cannot begin to solve the unconstrained localization problem. A single-axis vector component magnetometer loses the total-field sensor's motion-noise immunity, without providing any advantage in localization ability.

# Report Documentation Page

| Report Date | Report Type | Dates Covered (from... to) |
|---|---|---|
| 25FEB2002 | N/A | - |

| | |
|---|---|
| **Title and Subtitle**<br>Magnetic Detection and Tracking of Military Vehicles | **Contract Number** |
| | **Grant Number** |
| | **Program Element Number** |
| **Author(s)** | **Project Number** |
| | **Task Number** |
| | **Work Unit Number** |
| **Performing Organization Name(s) and Address(es)**<br>Quantum Magnetics, Inc. San Diego, CA 92121 | **Performing Organization Report Number** |
| **Sponsoring/Monitoring Agency Name(s) and Address(es)** | **Sponsor/Monitor's Acronym(s)** |
| | **Sponsor/Monitor's Report Number(s)** |

**Distribution/Availability Statement**
Approved for public release, distribution unlimited

**Supplementary Notes**
Papers from 2001 Meeting of the MSS Specialty Group on Battlefield Acoustic and Seismic Sensing, Magnetic and Electric Field Sensors, Volume 1: Special Session held 23 Oct 2001. See also ADM001434 for whole conference on cd-rom., The original document contains color images.

**Abstract**

**Subject Terms**

| | |
|---|---|
| **Report Classification**<br>unclassified | **Classification of this page**<br>unclassified |
| **Classification of Abstract**<br>unclassified | **Limitation of Abstract**<br>UU |

**Number of Pages**
13

A three-axis magnetometer triples the information originating from a single measurement point. However, it remains insufficient to localize a target.

In principle, two three-axis magnetometers with an overlapping field of view produce six independent measurements simultaneously, allowing a full solution. Symmetries of the magnetic dipole field mean that a third magnetometer, not collinear with the other two, must also detect the target in order to eliminate multiple solutions (called "ghosts"). Such arrays of sensors must communicate their data to each other or to a processing node in order to obtain a target solution.

Applications exist where internode communication is not feasible. "Smart" mines represent one such application: robustness and low cost dictate the independence of each munition. The Army's Next Generation Scatterable Mine (NGSM) program seeks to develop a new mine that can replace traditional antitank mines with a munition that allows the U.S. to sign the Ottawa Accords banning antipersonnel landmines.

When internode communications are disallowed, each node must independently locate and characterize a target. A magnetic tensor gradiometer provides a means to do so. A gradiometer takes the spatial derivative of the ambient field. Since the magnetic field has three components $B_i$, each of which can be differentiated with respect to three coordinates $x_j$, the field gradient is a tensor with nine elements, $\partial B_i/\partial x_j$.

Gradiometers offer advantages and limitations compared to magnetometers. In a spatially uniform field, the noise response to orientation changes is suppressed. Interference from distant sources is suppressed, since the dipole field gradient decays as $1/r^4$. Of course, this also presents a limitation in target detection range. A further limitation is described next.

Maxwell's Equation $\nabla \bullet \boldsymbol{B} = 0$ says that the trace of the gradient tensor is zero, so two of the diagonal terms determine the third. Furthermore, in free space, Maxwell's equation $\nabla \times \boldsymbol{B} = 0$ says that the tensor is symmetric, so three of the off-diagonal terms determine the other three. Thus, only five of the nine components provide independent information. In practical terms, this means that measuring the gradient alone will give the bearing toward the target and the orientation of the target's magnetic moment vector.[1] The fifth solved variable conflates the target's moment magnitude $M$ and its range $R$ into the single quantity $M/R^4$. This is called the "range-moment ambiguity" problem. Inversion of the gradient equations[1] yields four possible solutions for the target bearing and moment orientation, of which three are ghosts.

Attaining a truly useful individual sensor node requires the tensor gradiometer output as well as the local magnetic field vector output. We have shown that the resulting eight independent pieces of information suffice to eliminate ghost solutions (in all but a very few special cases) and to eliminate the range-moment ambiguity.

## 3.0 DETECTION AND TRACKING RANGE AS A FUNCTION OF NOISE

A recent paper[2] parameterizes the problem of detecting and tracking objects magnetically. The magnetic moment of a paramagnetic object can be expressed by the relation $M = KD^3$, where $D$ is the object's largest dimension and $K$ is an orientation-dependent demagnetization factor.

---

[1] W. M. Wynn, "Detection Localization, and Characterization of Static Magnetic Dipole Sources," in *Detection and Identification of Visually Obscured Targets*, C. E. Baum, Editor (Taylor & Francis, Philadelphia, 1999), pp. 337-374.

[2] A.R. Perry, P.V. Czipott, Y. Dalichaouch and D.O. Walsh, "Magnetic Localization and Real-Time Tracking of Concealed Threats," *Proc. SPIE* **4491**, in press, 2001.

A measurement occurs against a noise background. In the case of magnetic measurements, both environmental and instrumental noise sources can be modeled as a sparse array of uncorrelated time-varying dipoles $M_N = K_N D_N^3$, each at a nominal distance $R_N$.

The effective noise $N$ in a magnetometer measurement is given by $N = M_N/R_N^3$, where $N$ is taken over the same bandwidth as the individual uncorrelated signal measurements $S$ that form the data time series. Since the target's magnetic field decays as the inverse cube of distance, the noise and target characteristics directly determine the maximum range at which the object can be seen:

$$R_{B,max} \leq D(K/N)^{1/3} \tag{1}$$

This confirms the intuitive result that the useful detection range of a magnetometer is proportional to the scale $D$ of a family of objects (with relatively uniform $K$) and to the inverse cube root of the noise in the measurement.

The case of a gradient measurement depends on the baseline $L$ of the gradiometer. The approximate gradient signal (actually a finite difference) $G = \delta B$ can be expressed as $G = -3BL/R$, with a similar expression for the differential noise $\delta N$. We find that the maximum detection range for a gradient measurement is given by

$$R_{G,max} \leq R_{B,max}^{3/4} R_N^{1/4} \tag{2}$$

Equations (1) and (2) allow us to determine conditions under which an object is detected first in magnetic field or in gradient. Setting $R_{B,max} = R_{G,max}$, we find the condition

$$D_{crit} = R_N(N/K)^{1/3} \tag{3}$$

The critical scale length $D_{crit}$ corresponds to a fraction $(N/K)^{1/3}$ of the distance to the nearest equivalent noise source. Objects whose scale length $D$ exceeds $D_{crit}$ will be detected first in magnetic field. Objects with $D < D_{crit}$ will be detected first in magnetic gradient. Independently of knowledge of the quantitative value of $D_{crit}$, the knowledge of which sensor modality detected the object first gives an instantaneous classification of the detected object as "large" or "small".

As shown in Section 2, tracking a target requires detection of signals by both magnetometer and gradiometer. Nevertheless, the parameterization is useful in defining sensor configurations for other applications, such as magnetic trip wires. It shows that in applications involving small targets, using gradiometers may actually be advantageous, compared to magnetometers.

## 4.0 MAGNETORESISTIVE GRADIOMETERS

The NGSM application requires a low-power, low-cost, moderate-resolution sensor technology that can fit into a restrictive form factor. Magnetoresistive (MR) sensors, being small, integrated, thin-film devices, offer the hope to satisfy the form factor constraints. Quantum Magnetics has developed three generations of gradiometer using commercial MR sensors. Each of these has been tested in the field. The first gradiometer was a laboratory pre-prototype.[3] Figure 1 illustrates this unit in the laboratory.

[3] Y. Dalichaouch, A.R. Perry, B.R. Whitecotton, C.R. Moeller and P.V. Czipott, "Development of a room-temperature gradiometer system for underground structure detection and characterization," *Proc. SPIE* **4040** (*Unattended Ground Sensor Technologies and Applications II*, ed. E. Carapezza and T. Hintz), 74-82, 2000.

**Figure 1.** The laboratory prototype MR gradiometer (on circular plate); a fluxgate gradiometer with 30 cm baseline (triangular sensor) provides scale. Each "flux cube" structure surrounds three orthogonally oriented MR magnetometers. The gradiometer electronics board is visible in the background.

Each set of three MR magnetometers is enclosed in a set of orthogonal applied-field coils called a "flux cube". These coils null the ambient field, allowing each sensor to operate in a low-field environment. The current values used to null the field are determined by the reference sensor, at the center of the array. Gradient terms are formed by taking differences between sensors located at the corners of the triangular array. Note that the gradient tensor can be fully determined using a planar sensor layout, thanks to the tensor's symmetry and zero trace.

A special electronics unit operates the gradiometer. The operation is controlled by a Digital Signal Processing (DSP) chip and associated programmable logic array chip. Analog sensor voltages, conditioned by circuits on boards protruding from each flux cube, are digitized on the main electronics board. Feedback, modulation, and other analog control signals are generated by the DSP, routed through digital-to-analog converters, and sent to the flux cube coils and the sensors. The DSP also sends data through a serial link to a laptop computer. The RS485 current link allows an extended cable run; it is converted to RS232 before entering the laptop's serial port.

This unit was deployed at Picatinny Arsenal in July and August, 2000 and took the first data demonstrating tracking of military vehicles.

A fieldable gradiometer was fabricated and delivered to the Army in the same year (Figure 2). It reduced the separation between individual three-axis magnetometer units to a distance compatible with NGSM form factor constraints. The layout has been changed from a triangular array (with the reference sensor at the centroid) to a square array (with the reference on the perimeter). It also rendered the system more rugged and easier to deploy. Obviously, the entire unit remains far too large for the NGSM. In particular, the flux cubes are bulky and power-hungry. The electronics remain powered by AC line voltage. Nevertheless, the unit demonstrates that the gradiometer can function usefully with a reduced separation between sensors.

During 2001, Quantum Magnetics developed and deployed a third-generation system. This system dispenses with the flux cubes, relying on field coils integrated in each sensor die to null ambient fields at that sensor. In this operating mode, each sensor operates in a low field along its sensitive axis, but in ambient fields orthogonal to that axis. This operating mode is made possible by a new sensor die layout

that reduces the dependence of sensor gain on the off-axis ambient field. That nonlinearity had required the full flux cube configuration in earlier sensors.

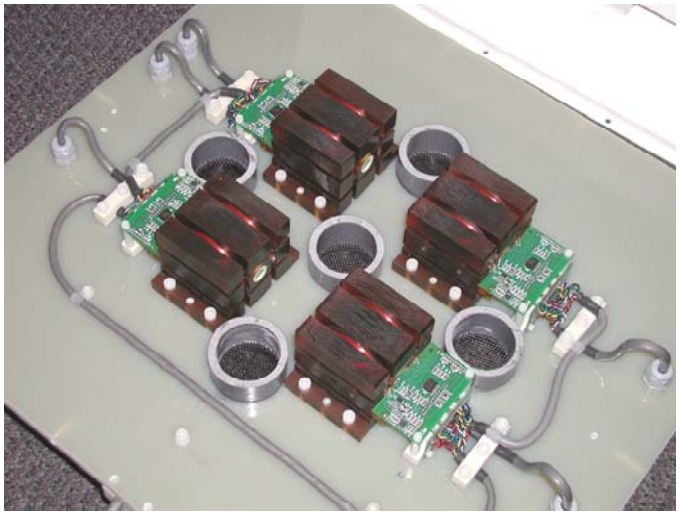

**Figure 2.** Field-ruggedized prototype gradiometer. Sensors lie on a circle of radius 20 cm. A cruciform array of vent holes provides thermal stabilization; exit vents are built into the weather-proof cover (not shown).

Figure 3 shows the latest gradiometer. The sensors reside on a circle 15 cm in diameter and fit entirely within a container 20 cm in diameter (the NGSM form factor requirement). In order to minimize development costs, the sensor boards were changed only minimally. The height of the assembly is thus a matter of short-term convenience, rather than the consequence of any fundamental requirement. It can be reduced substantially. The board on top serves purely an electrical interconnect function, at present. Most of the electronics currently on each sensor board can be migrated to the top board in a future design iteration.

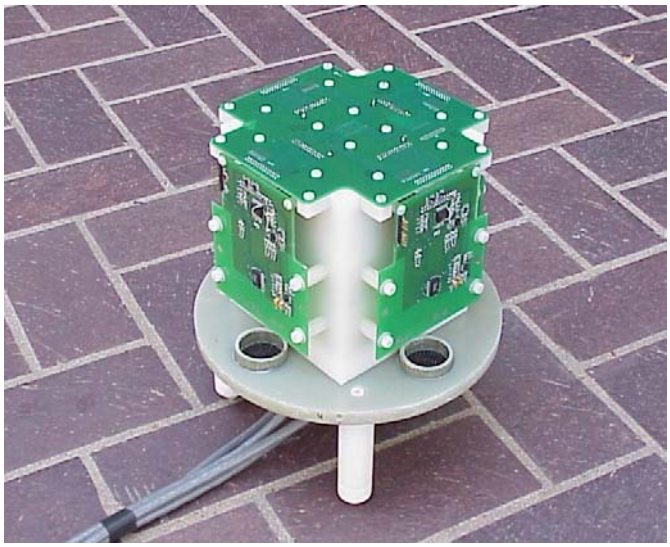

**Figure 3.** Latest MR gradiometer sensor head. Each vertical board holds three orthogonal MR magnetometers and associated signal conditioning circuits. The top board serves as an interconnect.

Figure 4 shows the housing of the main electronics board and of the batteries powering the present system. To minimize development costs, the electronics board was left unchanged from earlier versions. The sensor and electronics are housed in identical housings, also to conserve design and fabrication costs. The electronics board can easily be reduced to a <15 cm circular board form factor in a future iteration.

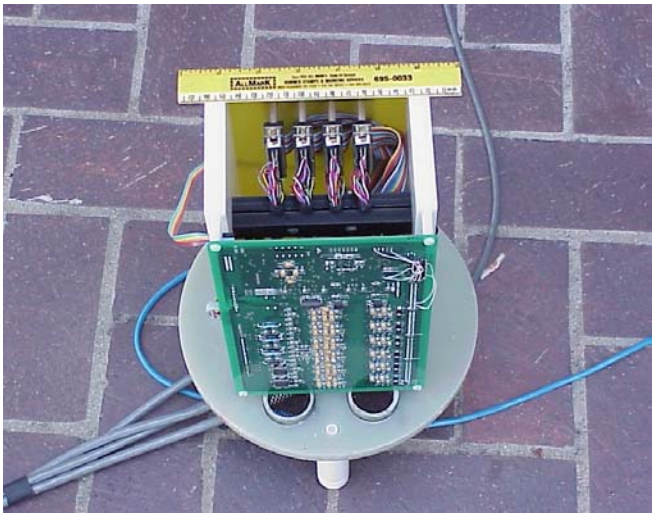

**Figure 4.** Main gradiometer electronics board. The board has twelve channels of 21-bit analog to digital converters, digital signal processing logic to monitor the sensors and generate control signals, and several channels of digital to analog converters to generate control currents. The board also streams resulting data to a computer via a serial RS-485 line (blue cable).

Figure 5 shows the entire system, with the sensor inside the cylindrical enclosure in the foreground, the electronics in the second cylindrical enclosure, and the battery in a black enclosure in the background. A blue cable runs from the electronics to the laptop computer, which is not visible in the photograph.

**Figure 5.** Overall system view showing the sensor enclosure (foreground), electronics enclosure (middle), and battery enclosure (rear). The photograph does not include the laptop computer, connected to the system via the blue cable running off the right side of the figure.

## 5.0 SIGNAL PROCESSING

One method to take gradient (and field) data and infer the location and moment of a target is to perform a deterministic inversion of the gradient equations. This is the basis of the Frahm-Wynn algorithm described extensively in reference 1. Inverting the gradient data alone gives rise to the ghost and range-moment problems described above. Including the field with the gradient eliminates the ghosts and resolves the range-moment ambiguity. In passing, we note that including the field is useful only when the sensor is stationary and stable, as motion-induced noise renders the field data unusable otherwise.

A second approach, the "matched filter" method, is probabilistic. Matched filtering usually entails correlating a measured sensor response against a set of hypothetical responses to find the best "match". Each hypothetical response is generated by forward computation of the known response for a particular set of source parameters.

With a static tensor gradiometer and magnetometer, we measure the magnetic field vector and field gradient tensor at a single location in space, and we wish to determine the location and orientation of a single magnetic dipole source. We know that range (distance to the source) only affects the magnitude of the gradient measurement. So we can reduce the set of hypothetical source parameters to source bearing and orientation.

One matched filtering approach is to generate a set of normalized hypothetical gradient measurements spanning all conceivable combinations of source bearing and orientation. We would then correlate the actual measurement with each of these to find the best match. This sheer scale of this approach is costly in terms of computations and storage requirements.

An alternate approach, and the approach that we use, is to view the vector dipole source as the superposition of three orthogonal magnetic dipole components, say $M_x$, $M_y$ and $M_z$. For each hypothetical source bearing, three normalized "matched filters" are applied to detect the three orthogonal dipole components $M_x$, $M_y$ and $M_z$. The matched filter for $M_x$ is the expected tensor gradient measurement for a dipole aligned in the x-direction at the given bearing, normalized to unit energy.

This approach is conceptually similar to quadrature detection in spectral analysis. In quadrature detection, we correlate pairs of orthogonal sinusoids with the measured signal to determine the frequency, magnitude and phase of an unknown sinusoid. In our magnetic field gradiometry, we correlate triplets of orthogonal tensor gradients with the measured gradient to determine the bearing, scaled magnitude and orientation angle of an unknown magnetic dipole source. We then use he magnetic field to resolve the scaled gradient response into a specific range and moment.

We have found one important constraint for this approach: the orthogonal basis for the dipole components cannot be selected arbitrarily. A dipole oriented in the direction of the bearing vector produces a gradient that is $3^{1/2}$ larger in magnitude than a dipole oriented perpendicular to the bearing vector. For this reason, the orthogonal basis should be chosen such that one basis vector is aligned with the bearing vector. This choice of basis vectors produces a set of three orthogonal matched gradient filter vectors. The orthogonal condition of the matched filters ensures independent detection and estimation of the three dipole components. Apparently, this is a requirement for unbiased bearing estimation. Analytic proofs of these results are not yet available. However, the orthogonality of gradients produced by the described basis, and the absence of bias in the derived bearing estimates, have been consistently observed.

In practice, we divide the unit sphere around the sensor into pixels with a user-selected angular resolution in elevation and azimuth. We calculate the response to each moment triplet in each pixel. This computation is lengthy, but it only needs to be performed once, at setup. The results can be stored in

memory. The matched-filter algorithm that finds the pixel with the best fit to the data is a simple linear correlation algorithm that runs very quickly. Actually, four pixels (corresponding to the true solution and three ghosts) satisfy this match. Applying the same algorithm to the magnetic field data then eliminates the ghosts and defines the actual target range and moment.

The Frahm-Wynn algorithm is nonlinear. Like most nonlinear methods, it is extremely sensitive to errors in the data. Linear correlation methods like the matched filter approach appear more robust in the presence of noise and systematic error.

A statistical investigation of the error in bearing and range estimates as a function of signal to noise ratio (SNR) was carried out. The RMS bearing error is plotted in Figure 6 as a function of SNR and angle $\Phi$ between the moment and bearing vectors. The SNR is calculated here as the true tensor gradient magnitude divided by $3\sigma_n$, where $\sigma_n$ is the sensor noise level. (Gaussian (0, $\sigma_n$) noise was added to each of the nine gradient measurements.)

The RMS bearing error for a given SNR is best (lowest) when the moment and bearing vectors are orthogonal: $\Phi = 90°$. The RMS bearing error is worst when the moment and bearing vectors are co-axial: $\Phi = 0°$. Two asymptotic logarithmic models are also depicted in Figure 6. It appears that in the orthogonal case the RMS bearing error varies as $1/SNR$, while in the co-axial case the RMS error varies as $1/SNR^{1/2}$.

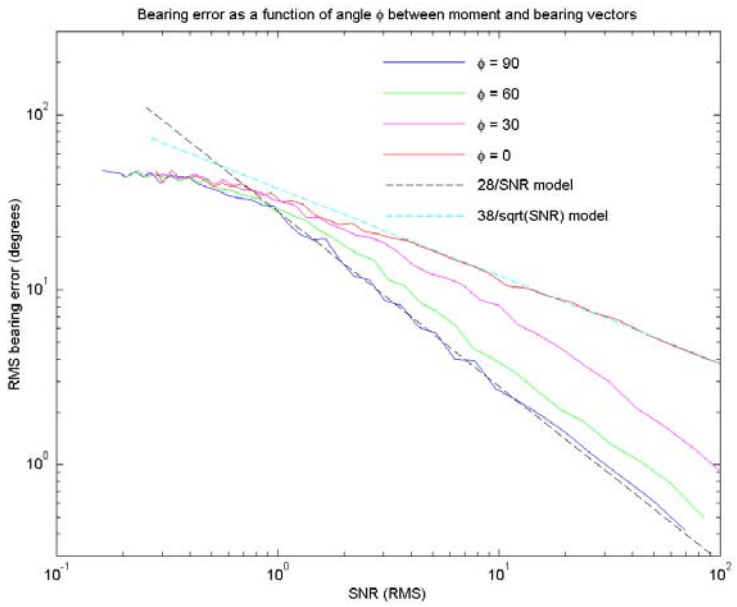


**Figure 6.** RMS bearing error as a function of both SNR and the angle $\Phi$ between the target moment and bearing vectors. Dashed lines represent empirical fits for two values of $\Phi$.

The mean range error is plotted as a function of SNR and $\Phi$ in Figure 7, where it is assumed that the moment magnitude is known exactly. The range tends to be systematically underestimated as SNR decreases. This is because the range estimate is inversely proportional to the measured gradient magnitude. At low SNR values, the gradient magnitude is over-estimated due to the noise contribution.

The standard deviation of the range error is plotted as a function of SNR and $\Phi$ in Figure 8. The standard deviation of the range error introduced by noise is negligible for SNR values greater than 1.

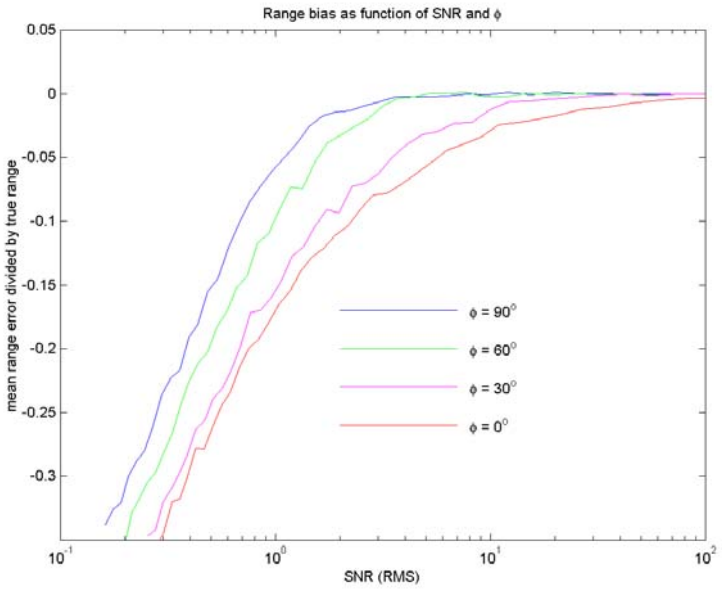


**Figure 7.** Mean range error, normalized to the true target range, as a function of SNR and the angle Φ between the target moment and target bearing.

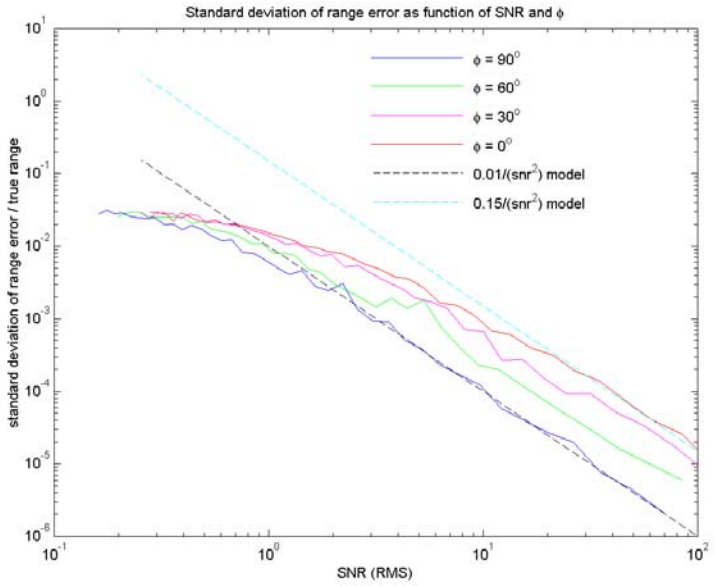


**Figure 8.** Standard deviation of the range estimate, normalized to the true target range, as a function of SNR and the angle Φ between the target moment and target bearing. Dashed lines represent empirical fits for two values of Φ.

## 6.0 FIELD RESULTS

The first-generation MR gradiometer of Figure 1 was deployed at Picatinny Arsenal for a data collection exercise in July and August, 2000. A fluxgate gradiometer was also deployed for comparison. Figure 9 shows the sensor in the field.

**Figure 9.** The laboratory MR gradiometer (front), its electronics (center left), and its AC power supply (on box on tarp), deployed next to the road at a remote site on the grounds of Picatinny Arsenal. A laboratory fluxgate gradiometer and its electronics are deployed in the background.

Although the experimental site was reasonably remote from human structures that can generate magnetic interference, we found that the local geology was itself highly magnetic (Figure 10). The site was on a mountain that has a high concentration of hematite and magnetite ores. The magnetization of the rock leads to appreciable background gradients, and its magnetic permeability leads to distortions of a target's magnetic field.

**Figure 10.** Pebbles and soil grains adhering magnetically to a bar magnet. The magnetized fragments are representative of approximately 50% of the overburden disturbed by the passage of a vehicle at the Picatinny Arsenal test site.

Measurements showed that estimates of target elevation were indeed seriously affected by the geology, but that estimates of target azimuth were acceptable. Figure 11 shows the track of a heavily armored military vehicle as it drove past the sensor. The vehicle's track was roughly a straight line heading toward magnetic north, then reversing course to the origination point. The figure, based on gradient data alone, shows four possible target tracks, of which one is correct and three are ghosts. In this analysis, the range-moment ambiguity was resolved by using the point of closest approach to calibrate the magnetic moment magnitude in post-processing. In this figure, the true track is the one that is largely vertical, on the right-hand side of the figure.

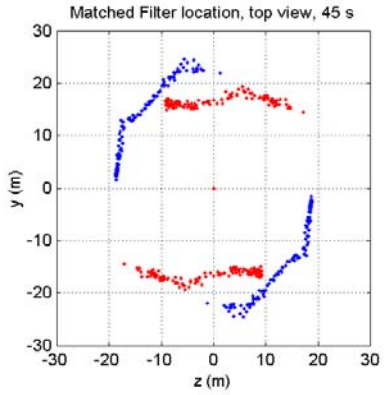


**Figure 11.** Estimated track of a heavily armored vehicle moving past the gradiometer, which was located at the origin. The true track of the vehicle starts at approximately $y$ = -20 m, $z$ = 20 m, heads up along $z$ = 20 m until $y$ = 0, and reverses course to the starting point. The lower right-hand track is the true solution, and the other three are the ghosts obtained in gradient-only processing. The estimated tracks curve back toward the sensor at longer range, as explained below.

The figure shows that azimuth estimates are reasonably consistent with reality, but that the range is systematically underestimated when the signal to noise ratio is small (< 3). At the longer tracking ranges, the path appears to curve around the sensor rather than continuing in the straight line of the actual path. The spurious curvature comes about at low signal to noise ratios, because the additive noise makes the target signal appear larger than it really is. As a result, the target appears to be closer than it really is. In principle, this effect is corrigible in the signal processing, by applying a range correction that is an empirically derived function of the estimated signal to noise ratio of a given measurement. Efforts to implement this correction factor have not yet yielded satisfactory results.

A comparison between the Frahm-Wynn and matched filter algorithms is provided by the track of a bar magnet being carried in a circular path around the gradiometer. Figure 12 shows that the track produced by the matched filter algorithm is less scattered; both algorithms yield distorted circles. The distortions may be caused by the magnetic geology of the site, or by calibration errors in the sensor.

In preparation for field tests performed in 2001, we implemented the full gradient-plus-field signal processing and have demonstrated that it eliminates both the ghost solutions and the range-moment ambiguity. Figure 13 illustrates the estimated path of a heavy-armor vehicle, using the system of Figure 5. The path can be obtained in real time and yields an unambiguous location of the target. The target path is accurate at short range (≤10 m), despite the fact that the field site chosen for this test lies atop the rebar-infested remains of a leveled building. The algorithm also calculates a munition firing solution at or near the closest point of approach (CPA).

Inspection of Figure 13 reveals several features. First, the estimated track curves back toward the sensor at the extremes of tracking range, as described above. Second, the elevation estimate is distorted, possibly by the presence of ferrous steel rebar under the sensor. Third, the track becomes heavily distorted just as the vehicle passes the CPA. The reasons for this are not yet definitively known. However, plausible explanations include (a) the effect of subsurface rebar, (b) the effect of the target's

magnetic multipoles at very close range, and (c) the effect of imperfect gradiometer calibration and balancing. Work is underway to explain and mitigate this effect.

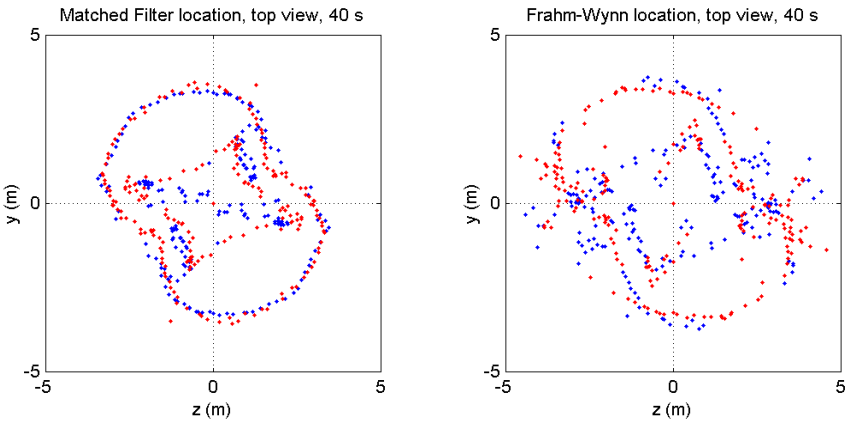


**Figure 12.** Estimates of the track of a magnet being carried in a circular track around the gradiometer. Two of the ghost tracks form the interior diamond shapes. The true track and its ghost, a reflection through the origin, form two distorted circles. The matched filter estimates, left, show less scatter than the Frahm-Wynn estimates, right.

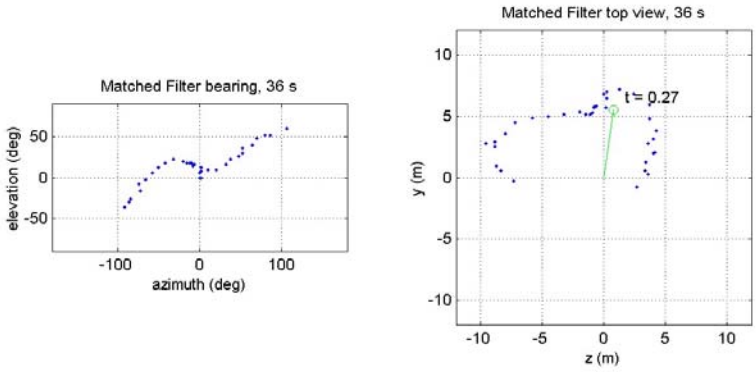


**Figure 13.** Real-time track of a heavily armored vehicle driving past the sensor, which was located at the origin. The true path of the vehicle was horizontal, left to right along a line represented by $y = 5$ m. The estimated track shows the expected distortion at longer ranges, converging on the true path at around 8 m range. The line radiating from the origin terminates at the firing solution determined by the algorithm.

## 7.0 STRENGTHS AND LIMITATIONS

The main advantage of magnetic gradiometry, compared to most other detection and tracking modalities, is that it is not limited to line-of-sight tracking. It can hence operate under all weather conditions, in the presence of heavy foliage, behind rocks or other structures (as long as they are not magnetically permeable, themselves), and the like. Another key advantage is that it is a completely passive modality and thus one with a low probability of being detected. Balanced against this are some inherent limitations of magnetic sensing, among them the following:

1. Gradiometry is inherently a short-range method, since the signal decays as the inverse fourth power of distance. Unlike radar, which suffers a similar range dependence, one cannot increase the power of a transmitted signal to increase range, since magnetic gradiometry is a passive method. Only improving the signal to noise ratio (SNR) can increase range, and then only weakly, as the fourth root of SNR. SNR improvements can arise from sensor technology improvements and from detection and localization algorithm improvements.

2. The accuracy and effectiveness of magnetic target tracking in an urban environment, where ferrous objects are not confined below the ground surface, remains to be determined. Field studies to date indicate that target azimuth estimates are robust against the presence of magnetically permeable bodies underground, as long as they are either diffuse (e.g., geological structures) or relatively small and scattered (e.g., steel rebar).

3. Since a single tensor gradiometer and magnetometer yield only eight independent data points per measurement, the sensor can only give an accurate location for one target at a time. If two or more targets generate equivalent signals, the sensor will calculate a location as though only a single target were present. In practice, the strong range dependence of the signal means that only a single target dominates the signal at any time, mitigating this limitation.

In addition to the generic limitations of magnetic gradiometry are a few problems identified with the prototype systems described herein. These are:

1. Small calibration errors in the gradiometer, known as “gradiometer imbalance”, have not yet been resolved. These errors not only raise the noise floor of the gradient measurements, but also introduce systematic errors in target localization. These errors can be complicated functions of target position, leading to path distortions of the type observed in Figure 9. Calibration errors become proportionately more important as the baseline decreases. Work is proceeding to resolve these residual errors.

2. A problem in the electronics results in intermittent impulsive noise spikes. The nature of the problem has not been conclusively identified, but is being sought, at the time of writing.

Solving these two problems should yield a substantial improvement in both the accuracy of estimated tracks and the range at which the tracks are acquired. Anticipated improvements in tracking range are in the range of several to many tens of percent.

Further work in signal processing algorithms may also yield similar performance improvements. Means of suppressing both coherent and incoherent noise are under active investigation by our group and others.

Magnetic gradiometry promises a robust means to detect and track military vehicles. Several obstacles to practical implementation have been addressed and resolved, partially or completely. Resolving the remaining obstacles appears feasible.